Los Alamos
NATIONAL LABORATORY
EST. 1943

Environmental Programs
P.O. Box 1663, MS M991
Los Alamos, New Mexico 87545
(505) 606-2337/FAX (505) 665-1812

National Nuclear Security Administration
Los Alamos Site Office, MS A316
Environmental Restoration Program
Los Alamos, New Mexico 87544
(505) 667-4255/FAX (505) 606-2132

Date: March 9, 2009
Refer To: EP2009-0117

James P. Bearzi, Bureau Chief
Hazardous Waste Bureau
New Mexico Environment Department
2905 Rodeo Park Drive East, Building 1
Santa Fe, NM 87505-6303

Subject: Submittal of the Numerical Analysis of the Material Disposal Area G Soil-Vapor Extraction Test

Dear Mr. Bearzi:

Enclosed please find two hard copies with electronic files of the Numerical Analysis of the Material Disposal Area G Soil-Vapor Extraction Test. This report is referenced in the Pilot Test Report for Evaluating Soil-Vapor Extraction at Material Disposal Area G at Technical Area 54, Revision 1, and helps to better define the radius of influence from the Material Disposal Area (MDA) G soil-vapor extraction (SVE) pilot test. It also helps to support the conclusion that the SVE test at MDA G was effective in removing subsurface volatile organic compounds.

If you have any questions, please contact Steve Paris at (505) 606-0915 (smparis@lanl.gov) or Ed Worth at (505) 606-0398 (eworth@doeal.gov).

Sincerely,

B-G Schappell for MJG

Michael J. Graham, Associate Director
Environmental Programs
Los Alamos National Laboratory

Sincerely,

Edwin P. Worth for

David R. Gregory, Project Director
Environmental Operations
Los Alamos Site Office

MG/DG/DM/SP:sm

Enclosures: 1) Two hard copies with electronic files - Numerical Analysis of the Material Disposal Area G Soil-Vapor Extraction Test (LA-UR-09-0995)

Cy: (w/enc.)
Neil Weber, San Ildefonso Pueblo
Ed Worth, DOE-LASO, MS A316
Steve Paris, EP-CAP, MS M992
RPF, MS M707 (with two CDs)
Public Reading Room, MS M992

Cy: (Letter and CD only)
Laurie King, EPA Region 6, Dallas, TX
Steve Yanicak, NMED-OB, White Rock, NM
Phil Stauffer, EES-16, MS T003
Kristine Smeltz, WES-DO, MS M992
EP-CAP File, MS M992

Cy: (w/o enc.)
Tom Skibitski, NMED-OB, Santa Fe, NM
Keyana DeAguero, DOE-LASO (date-stamped letter emailed)
Michael J. Graham, ADEP, MS M991
Alison M. Dorries, WES-DO, MS M992
Dave McInroy, EP-CAP, MS M992
IRM-RMMSO, MS A150 (date-stamped letter emailed)

LA-UR-09-0995
March 2009
EP2009-0117

Numerical Analysis of the Soil-Vapor Extraction Test at Material Disposal Area G, Technical Area 54

Los Alamos
NATIONAL LABORATORY
EST. 1943

Prepared by the Environmental Programs Directorate

Author: Philip H. Stauffer, Ph.D., Hydrogeologist, EES-16

CONTENTS

Figures

Table

1.0 INTRODUCTION

The calculations presented in this report supplement the Material Disposal Area (MDA) G pilot test report (LANL 2008, 103902) and are designed to show that soil-vapor extraction (SVE) performed at MDA G is effective and conforms to the current conceptual model of vapor transport within the dry mesas of the Pajarito Plateau, where Los Alamos National Laboratory (the Laboratory or LANL) is located. Previous SVE testing at MDA L, located approximately 1400 m to the west on Mesita del Buey (Figure 1.0-1), provides much information on how subsurface pore gas, including vapor contaminants, behaves in the rocks that make up the mesa. In particular, Stauffer et al. (2007, 097871) contains a detailed summary of numerical analysis of the MDA L SVE pilot test that is beyond the scope of the current report. The MDA L SVE analysis is based on more than 15 yr of research into a vapor-phase volatile organic compound (VOC) plume at MDA L and covers plume nature, extent, and possible future behavior (see section 2.3 of LANL 2007, 099777). Results from this work can be found in the following references: (Neeper 2002, 098639; Stauffer et al. 2005, 090537; Stauffer et al. 2005, 097432; Stauffer et al. 2007, 104950; Stauffer et al. 2007, 097871; Vrugt et al. 2008, 104951). The fundamental scientific findings from the analyses performed for MDA L provided the foundation for the limited numerical analysis of the MDA G SVE pilot test presented in this report.

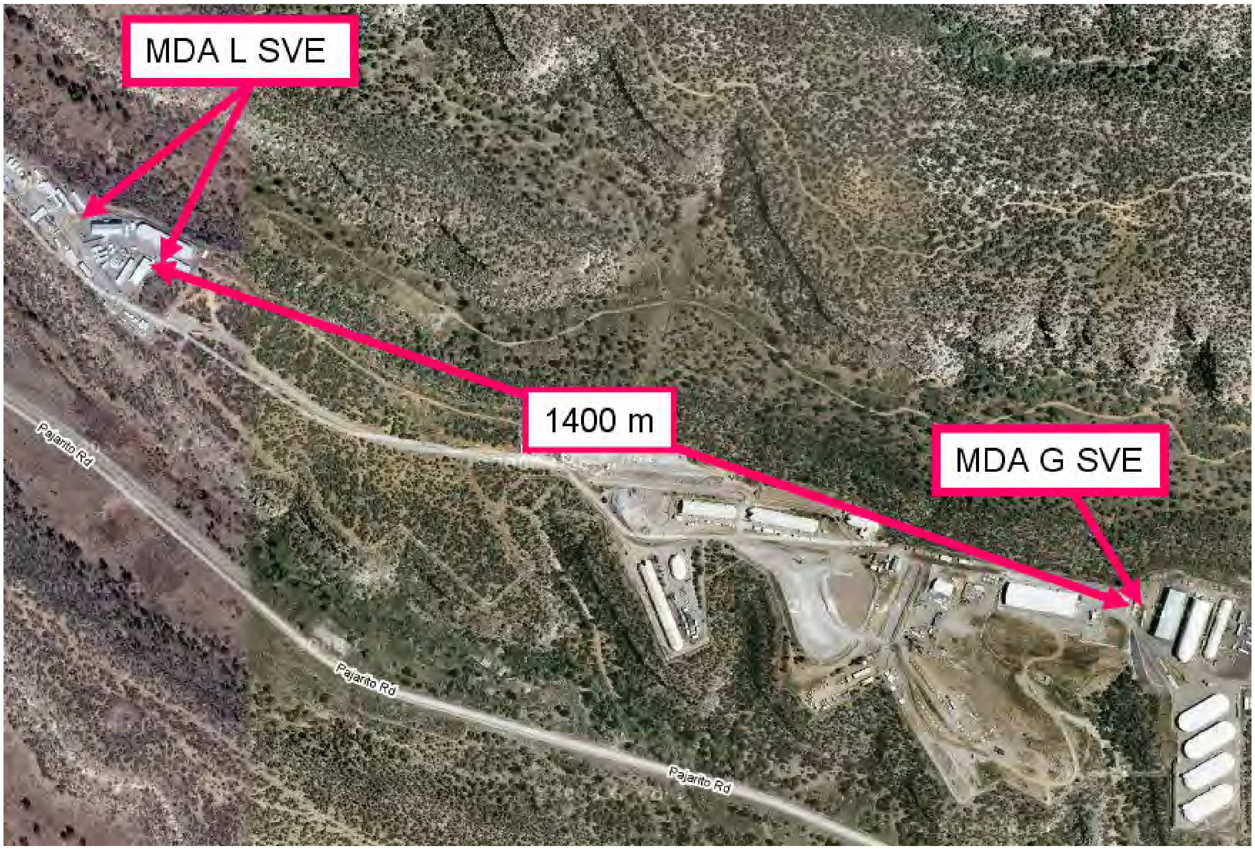

Figure 1.0-1 Location of the MDA G SVE pilot test relative to the MDA L SVE pilot test

The goal of the MDA G SVE pilot test was to evaluate the effectiveness of SVE at this site. Figure 1.0-2 shows the location of the shallow and deep SVE boreholes at MDA G and includes several of the surrounding boreholes that were used to monitor changes in pressure and concentration during the testing. The original Revision 0 submittal of the MDA G SVE pilot test report (LANL 2008, 103902) described the test and qualitative measures that showed that the shallow test was effective in removing VOCs from the subsurface. Additional information has been requested by the New Mexico Environment Department (NMED) to include the relationship between applied suction and flow rate in the shallow and deep SVE tests and the approximate radius of influence (ROI) of the shallow SVE test (NMED 2008, 104275). These additional results help provide a quantitative confirmation that SVE is effective at MDA G.

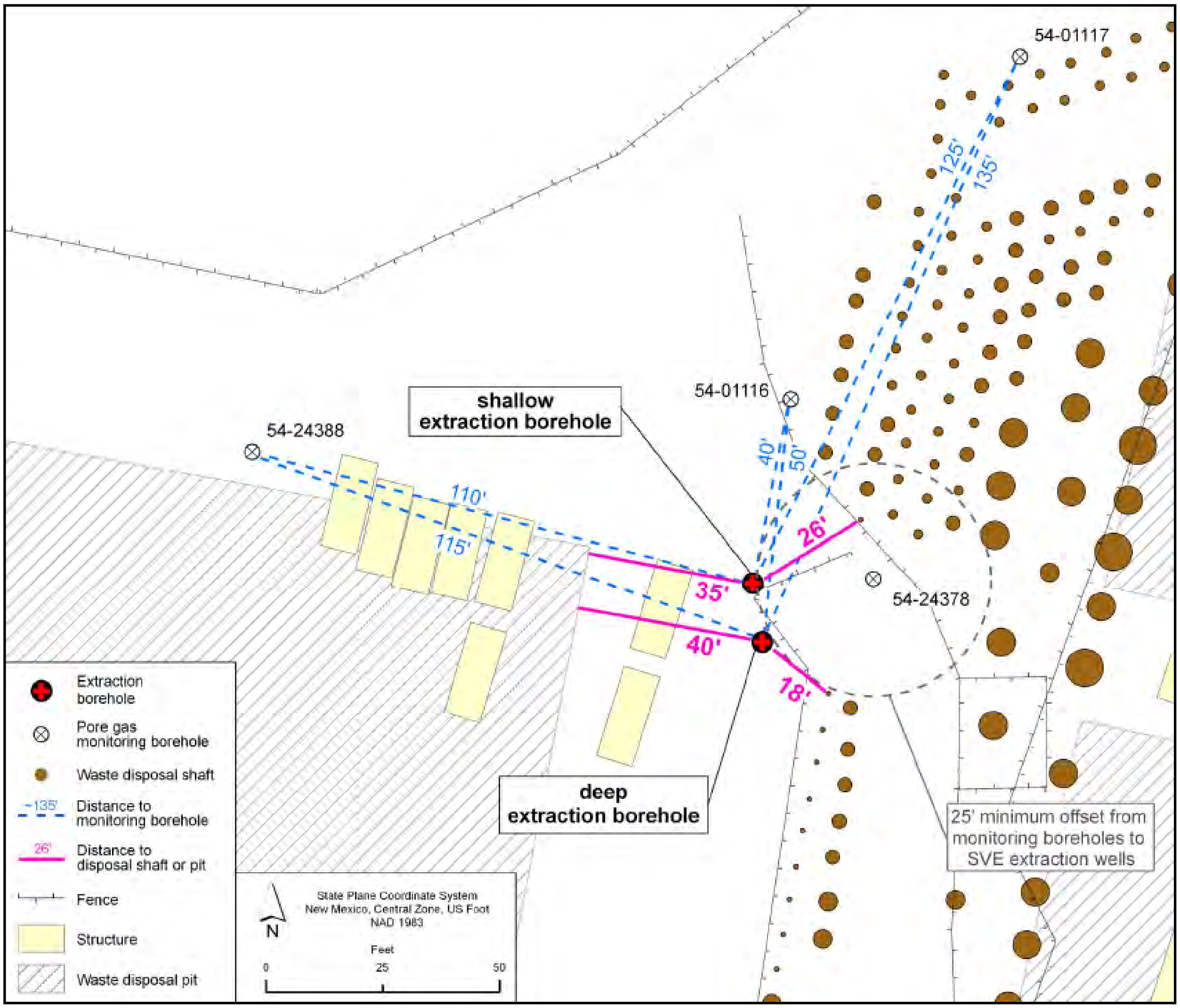

Notes: Based on Figure 3.2-4 of the MDA G SVE pilot test report (LANL 2008, 103902). Also shown are surrounding boreholes (54-24378, 54-24388, 54-01116, and 54-01117) in which pressure and VOC concentration data were collected.

Figure 1.0-2 Locations of the shallow and deep SVE test boreholes

2.0 NUMERICAL MODEL DESCRIPTION

In the following sections, a radially symmetric two-dimensional (2-D) numerical model of both the shallow and deep SVE tests is used to verify that the collected extraction data are consistent with previously determined values for the permeability of the geologic units in the subsurface of Technical Area 54. The model is run using the multiphase heat and mass transfer computer code FEHM (Zyvoloski et al. 1997, 070147). FEHM is continually verified against a host of test problems that ensure the code can accurately simulate a range of physical processes. The most important physical processes included in the current analysis are the flow of pore gas through the subsurface, contaminant transport, and the fractionation of VOCs from the vapor-phase into the liquid phase through Henry's law partitioning. The governing equations for these coupled processes are described in more detail in (Zyvoloski et al. 1997, 070147; Stauffer and Rosenburg 2000, 104952; Stauffer et al. 2007, 097871).

Once the domain is created and the boundary and initial conditions are applied, the first simulations performed are used to estimate bulk permeability of the rocks beneath MDA G. This step finds the permeability at which the simulated flow rate and suction match the field test using a single value of permeability for all geologic units. Next, the pore-gas permeabilities for the individual geologic units beneath MDA G are varied until both the shallow and deep tests yield the correct mass flow rate at the applied suction. This step is called model calibration. Next, the simulation results are compared with field data of pressure responses in nearby boreholes to show that the calibrated model can recreate pressure responses similar to the field-scale tests. This step is called field validation. Next, the calibrated model is used to describe the relationship between suction and flow rate in the shallow and deep extraction boreholes. Finally, simulations using the calibrated model are used to generate results that provide an estimate of the ROI of the shallow and deep SVE tests.

2.1 Model Domain, Boundary, and Initial Conditions

The domain used to simulate both the shallow and deep tests at MDA G is shown in Figures 2.1-1 and 2.1-2. The only differences in the domain between the two tests are the depth of the open interval and the length of the cased borehole. The geometry of the mesa was based on a topological map of MDA G and simplifies the slope of Cañada del Buey to a constant value. The domain is radially symmetric and because of the mesa's topographical relief, the simplified mesa has a conical shape. The use of radial geometry is required because the SVE test is fundamentally a radial problem, with extracted pore gas flowing toward the extraction borehole from all sides. The geologic units shown in Figures 2.1-1 and 2.1-2 are based on Figure 3.2-2 in the MDA G SVE pilot test report (LANL 2008, 103902), which shows the stratigraphy observed in the shallow SVE borehole. Based on Figure 3.2-3 of the MDA G SVE pilot test report, it is assumed that the same stratigraphy is appropriate for both tests (LANL 2008, 103902). More detail on the geologic units can be found in Stauffer et al. (2005, 090537) and references therein. The numerical mesh that underlies both Figures 2.1-1 and 2.1-2 begins with very small grid spacing at a radius of 0.0 to capture the 0.1-m radius of the borehole in the section of open hole. The grid spacing then increases as the radius increases such that there are 310 nodes in the radial direction spanning nearly 500 ft. Mesh spacing in the vertical direction is fixed at 0.5 m.

Material properties including porosity and saturation for the geologic units shown in Figures 2.1-1 and 2.1-2 were taken from Stauffer et al. (2007, 097871, Table II). The rocks at MDA G are quite dry and the bulk of the pore spaces is filled with pore gas, a mixture of air, water vapor, and any volatile contaminants that may be present. Values and justification for borehole permeability and casing permeability are also taken from Stauffer et al. (2007, 097871).

The model is initialized with a steady pore-gas pressure distribution fixed to a mesa top pressure at zero depth of 79 kPa. The model bottom pressure is fixed to the background static pressure of 79.554 kPa based on measured pressure response in the basalt at MDA L (Neeper 2002, 098639). Tracer concentration is fixed to zero in both the atmosphere and along the bottom boundary. The movement of liquid water is stopped through manipulation of the relative permeability functions. The shallow and deep SVE tests are simulated by applying the average measured suction to the top node of the simulated borehole and allowing subsurface pore gas to be pulled from the rocks into the borehole.

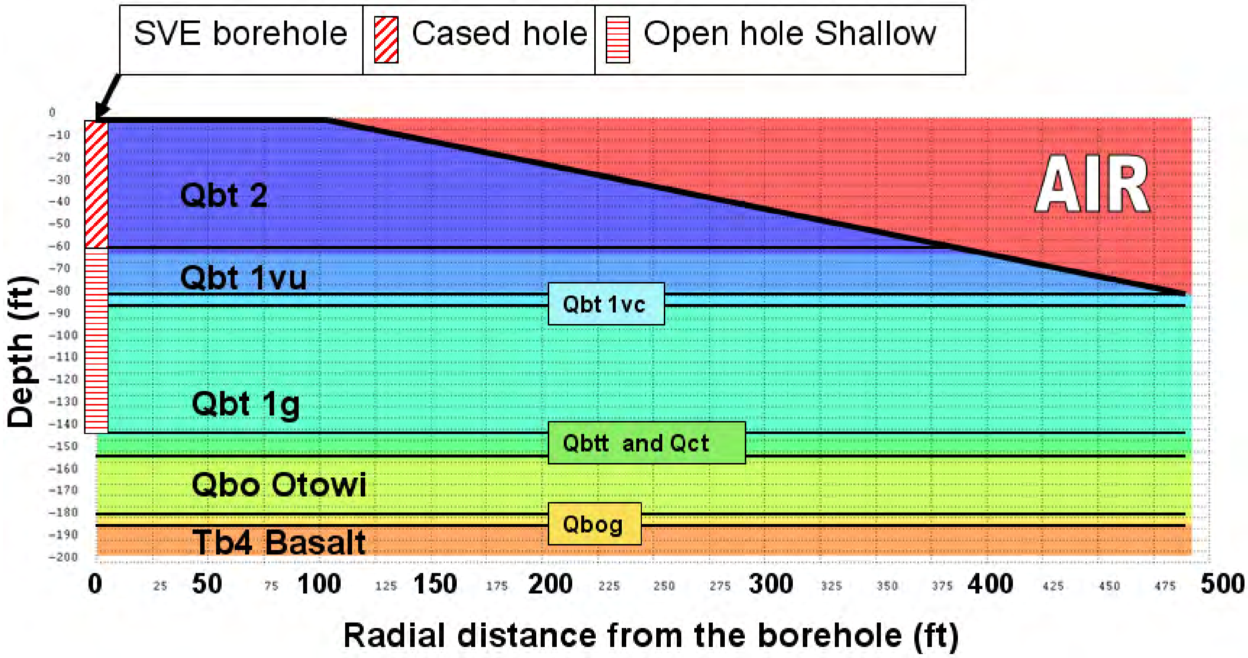

Figure 2.1-1 **Simplified stratigraphy and topography used for simulations of the MDA G shallow SVE pilot test**

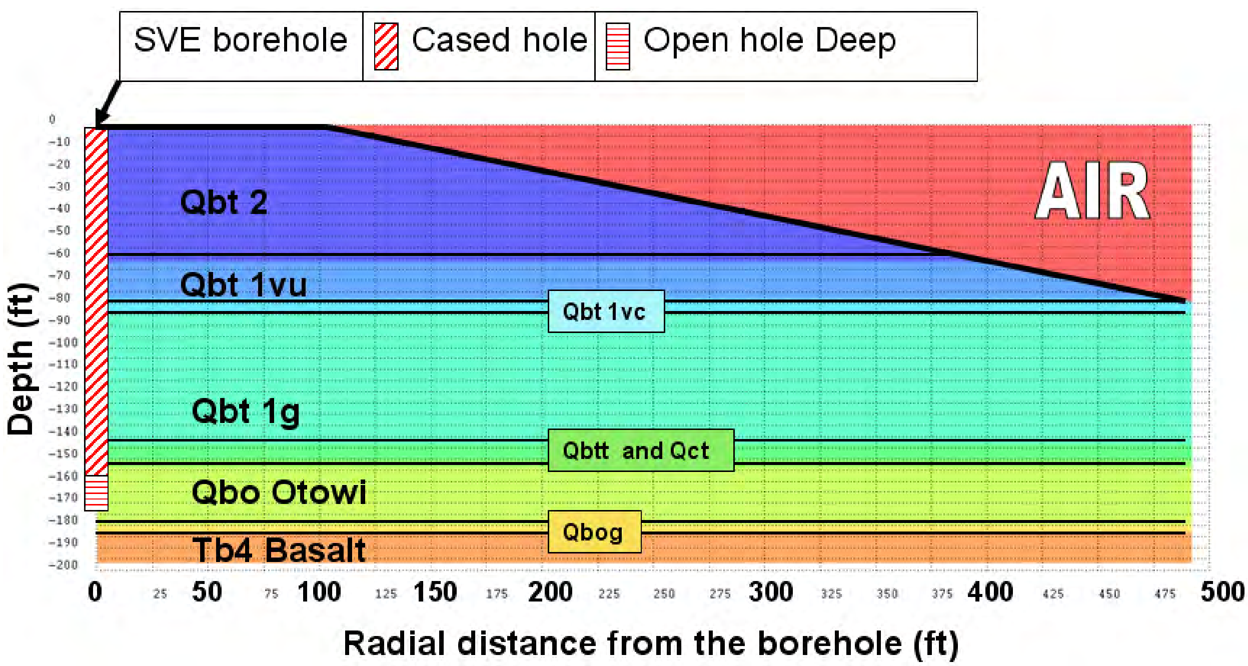

Figure 2.1-2 **Simplified stratigraphy and topography used for simulations of the MDA G deep SVE pilot test**

2.2 Estimate of Bulk Permeability

Although packer permeability data were collected at MDA G as part of the pilot test, problems with data processing did not allow realistic estimates to be calculated. Fortunately, the SVE test itself is a very sensitive test of the bulk or average permeability in the subsurface. For any specified suction at the top of the borehole, only one value of bulk permeability will lead to the correct flow rate of gas to the surface. Initial calculations that balanced the applied suction and observed flow rate showed that the bulk permeability in the subsurface at MDA G for the shallow test was on the order of a 6.5 darcies (6.5e–12 m^2), while for the deep test, the bulk permeability was closer to 1.3 darcies (1.3e–12 m^2). Bulk permeability measurements are useful, but they do not capture the known range of variability in the subsurface on Mesita del Buey. A very good demonstration of this is that the bulk permeabilities calculated for the shallow and deep tests are quite different. However, a numerical model of the site must contain both high permeability to fit the shallow test and lower permeability to fit the deep test. To capture this variability and because the geology at MDA G is very similar to MDA L, the mean packer permeabilities for the same geologic units at MDA L (Stauffer et al. 2007, 097871, Table III) were used as a starting point for simulations of the MDA G SVE pilot test (Table 2.2-1).

Table 2.2-1
Permeability Data from MDA L and Calibrated Permeability Values for the MDA G SVE Pilot Test

Geologic Unit	0.6-m Packer Permeability (includes fractures) (m^2)			Mean Core Permeability (matrix only) (m^2)	Calibrated Values for MDA G (m^2)
	Min	Mean	Max		
Qbt 2	5.3e-13	2.0e-13	3.8e-12	2.0e-13	4.47E-12
Qbt v(u)	4.7e-13	1.2e-13	1.6e-11	1.2e-13	7.61E-12
Qbt 1v(c)	8.5e-14	1.2e-13	1.2e-11	1.2e-13	3.95E-12
Qbt 1g	1.1e-13	1.3e-13	5.4e-11	1.3e-13	6.57E-12
Qbtt	9.3e-13	n/a[a]	1.7e-11	n/a	1.97E-11
Qct	1.2e-12	n/a	1.1e-11	n/a	1.50E-11
Qbo	5.5e-13	2.3e-13[b]	7.1e-13	2.3e-13[b]	1.31E-12
Qbog	n/a	n/a	n/a	n/a	1.42E-11
Tb 4 basalt	n/a	n/a	n/a	n/a	1.89E-11
Calculated bulk permeability for the shallow SVE test					6.5e-12
Calculated bulk permeability for the deep SVE test					1.3e-12

Notes: Based on Stauffer et al. (2007, 097871). 1 darcy = 1.e–12 m2.

[a] n/a = Not applicable.

[b] Cañada del Buey data.

2.3 Model Calibration

The calibration of the two tests to the permeability in Mesita del Buey was performed in an iterative manner. Because the deep SVE test is much more sensitive to the permeability of the Otowi Member (Qbo), the approximate permeability of the Otowi Member required to simulate the measured flow rate at the applied measured suction was calibrated first.

Next, the shallow SVE test was calibrated by increasing the pore-gas permeability of all geologic units above the Otowi Member by a constant fraction until the simulated flow rate for this test matched the data at the applied measured suction. Next, these values of permeability were used to simulate the deep SVE test, and the Otowi Member permeability was refined to regain the match of flow rate to suction. Finally, the resulting permeability values were rerun in the shallow SVE simulation, which led to results that were very close to the measured flow rate versus suction. The values of permeability that resulted from this stepwise calibration are shown in the last column of Table 2.2-1. These values generally fall between the mean and the maximum permeability values measured with packers on the same geologic units at MDA L (Neeper 2002, 098639). The final values of permeability resulted in a simulated flow rate of 105.1 scfm at a suction with 1.7 in. Hg (5.76 kPa) for the shallow SVE test and 16.7 scfm at a suction of 4.97 in.Hg (16.83 kPa) for the deep SVE test.

2.4 A Model Field-Validation Step

As presented above, the modeled permeability structure was calibrated simultaneously to the flow rate versus extraction data for both the shallow and deep SVE tests. It is feasible to analyze some model/data behavior to provide incremental validation steps, even though complete validation of subsurface flow models is difficult. To double-check, or validate that the numerical model of SVE at MDA G is in general agreement with the test data, one can look at the correlation between data and model results for changes in pressure measured in nearby boreholes. Figure 2.4-1 shows the pressure response of the modeled extraction tests in relationship to the measured pressure responses. Given the fact that the model geometry does not exactly reproduce the three-dimensional (3-D) mesa geometry, the simulations recreate the magnitude of decreasing drawdown with distance from the extraction boreholes for both the shallow and deep SVE tests. These results confirm that the model is able to recreate more than just the calibration correlation and provide an increased level of confidence that the simulations of SVE can be used to make decisions. Further refinement of the data/model correlation would require a more detailed 3-D model.

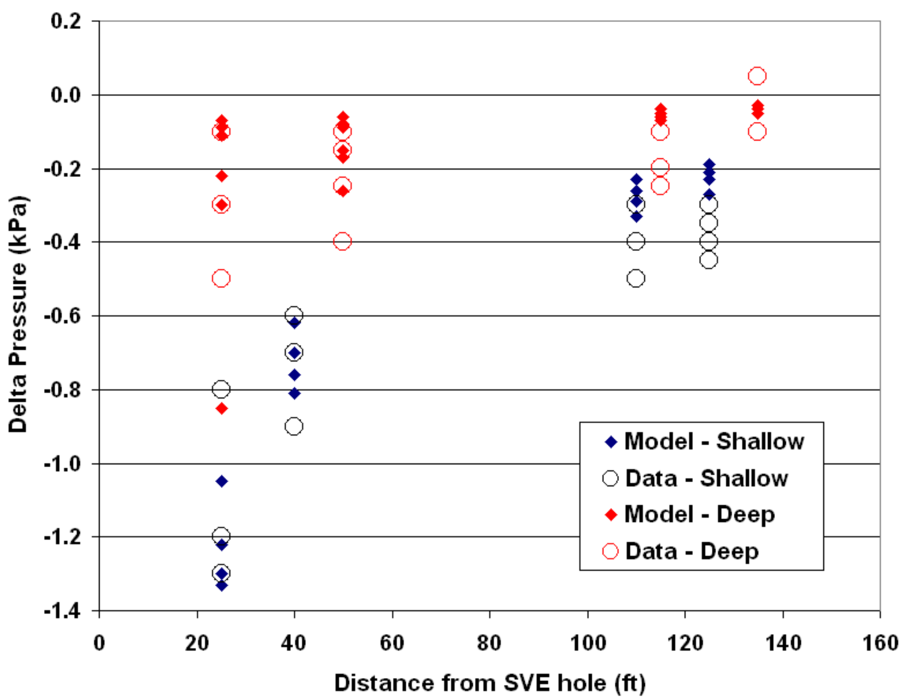

Figure 2.4-1 Simulated pore-gas pressure drawdown versus measured pore-gas pressure drawdown for both the shallow and deep tests in nearby monitoring boreholes

The calibrated numerical model can now be used to determine (1) the relationship between flow rate and suction and (2) the approximate radius of influence for both the shallow and deep SVE tests.

3.0 NUMERICAL MODEL RESULTS

3.1 Flow Rate Versus Suction

Figures 3.1-1a and b show how the flow rate in the simulated shallow and deep SVE tests varies as a function of suction at the top of the borehole. Included on these figures is the single data point from each of the SVE tests. As expected, the trend is nearly linear and provides model validation targets if further testing is done during the corrective measures evaluation and corrective measures implementation stages. The conversion from inches of mercury to kPa is given as 1 in. Hg = 3.387 kPa.

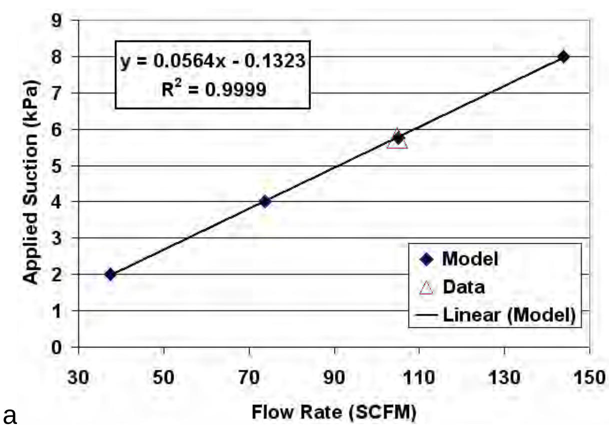

a

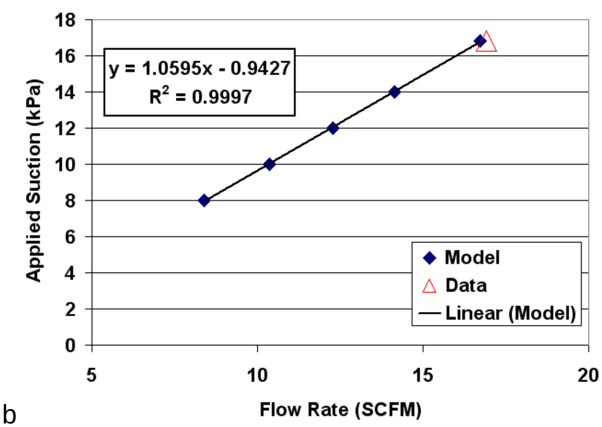

b

Figure 3.1-1 Flow rate versus suction for the (a) shallow and (b) deep SVE tests

3.2 ROI

The ROI in an SVE test can be a somewhat misleading concept. Because the pressure disturbance caused by the applied suction can reach quite far from the extraction borehole, the radius to which a pressure response propagates can be quite large. However, this does not mean that much is happening to the soil-gas located at such a large radius. Additionally, because the geologic units have different permeabilities, each geologic unit may have a separate ROI. Finally, the fact that the upper geologic units at MDA G outcrop along the canyon edges leads to an additional complicating factor. Acknowledging these difficulties, the U.S. Environmental Protection Agency (EPA) states:

> Design Radius of Influence (ROI) is the most important parameter to be considered in the design of an SVE system. The ROI is defined as the greatest distance from an extraction well at which a sufficient vacuum and vapor flow can be induced to adequately enhance volatilization and extraction of the contaminants in the soil. Extraction wells should be placed so that the overlap in their radii of influence completely covers the area of contamination." (EPA 2009, 104489)

Given a lack of a quantifiable definition that can be calculated, such as a radius at which the suction drops below a given value, one then uses numerical methods and simulations to determine the radius of influence for the MDA G SVE tests.

3.3 Shallow SVE Test ROI

The following figures show visually how pore gas within the simulated mesa moves in response to the shallow SVE suction by using a hypothetical tracer distributed in vertical bars. The hypothetical tracer has the same properties as 1,1,1 TCA (1,1,1 trichloroethane) and is fractionated between the pore water and the soil gas as described in Stauffer et al. (2005, 090537). Dispersivity and diffusion are both set to zero to reduce spreading and allow the pore-gas flow to be more easily visualized. The uniform bars of constant concentration are used here to estimate only ROI, not to represent the actual concentration in the mesa. The maximum extraction time of 60 d is based on analysis performed in Stauffer et al. (2007, 097871) to optimize the MDA L SVE system for remediation of the VOC plume at that site. This report assumes the same active extraction period because the calculated permeability values at MDA L are very similar to those calculated at MDA G.

Figure 3.3-1a shows the hypothetical tracer distribution that is initialized in the model. Concentration in each bar is initially uniform at 1 mole of tracer per kilogram of pore gas. The bars of concentration get wider with increasing radius because the numerical mesh gets coarser in this region. Concentration is fixed to zero in the region above the land surface and at the base of the model in the basalt.

Figures 3.3-1b–f show the progression of the simulated extraction at 3, 15, 30, 45, and 60 d after the test begins. In these figures, the effect of high permeability in Qbtt and Qct can be seen by movement of tracer at greater radius than in the overlying Qbt 1g. Likewise, the lower permeability Otowi Member shows less effect of the extraction at a given time. Interestingly, the initial tracer profile is disturbed to a radius of nearly 500 ft in the highly permeable units at only 30 d. However, as suggested by EPA guidance, this does not mean that the ROI is 500 ft. Figure 3.2-1f shows that by the end of 60 d, a conservative region of active extraction is limited to a radius of approximately 100–150 ft from the SVE borehole. The light blue concentration in this region is approximately 1/10th the original value.

To further constrain the ROI of the simulated shallow SVE test, single bars of concentration at fixed distance are simulated. These simulations show how the hypothetical tracer at a given distance is likely to respond over time with no interaction from tracer originating at other distances. Figure 3.3-2a shows that an initial C=1.0 bar at 150 ft is not fully extracted in 60 d. At 125 ft, a fixed initial bar is nearly removed (Figure 3.3-2b), while an initial bar at 100 ft is almost totally removed from the system in less than 60 d, as shown in Figure 3.3-2c.

Another way to look at the mass removal for the simulated shallow SVE test is to plot the fraction of mass remaining as a function of time. In Figure 3.3-3, one can see that the 100-ft bar is 80% removed by approximately 30 d, while by 60 d approximately 90% of the mass is removed. After 60 d, the mass in the bar at 150 ft is reduced to approximately 20% of its original mass; however, after 60 d the bar at 175 ft loses less than 50% of its original mass. Thus the ROI can conservatively be estimated to be on the order of 150 ft for the simulated MDA G shallow SVE test, with a suction of 1.7 in. Hg (5.76 kPa) for a period of active extraction spanning 60 d.

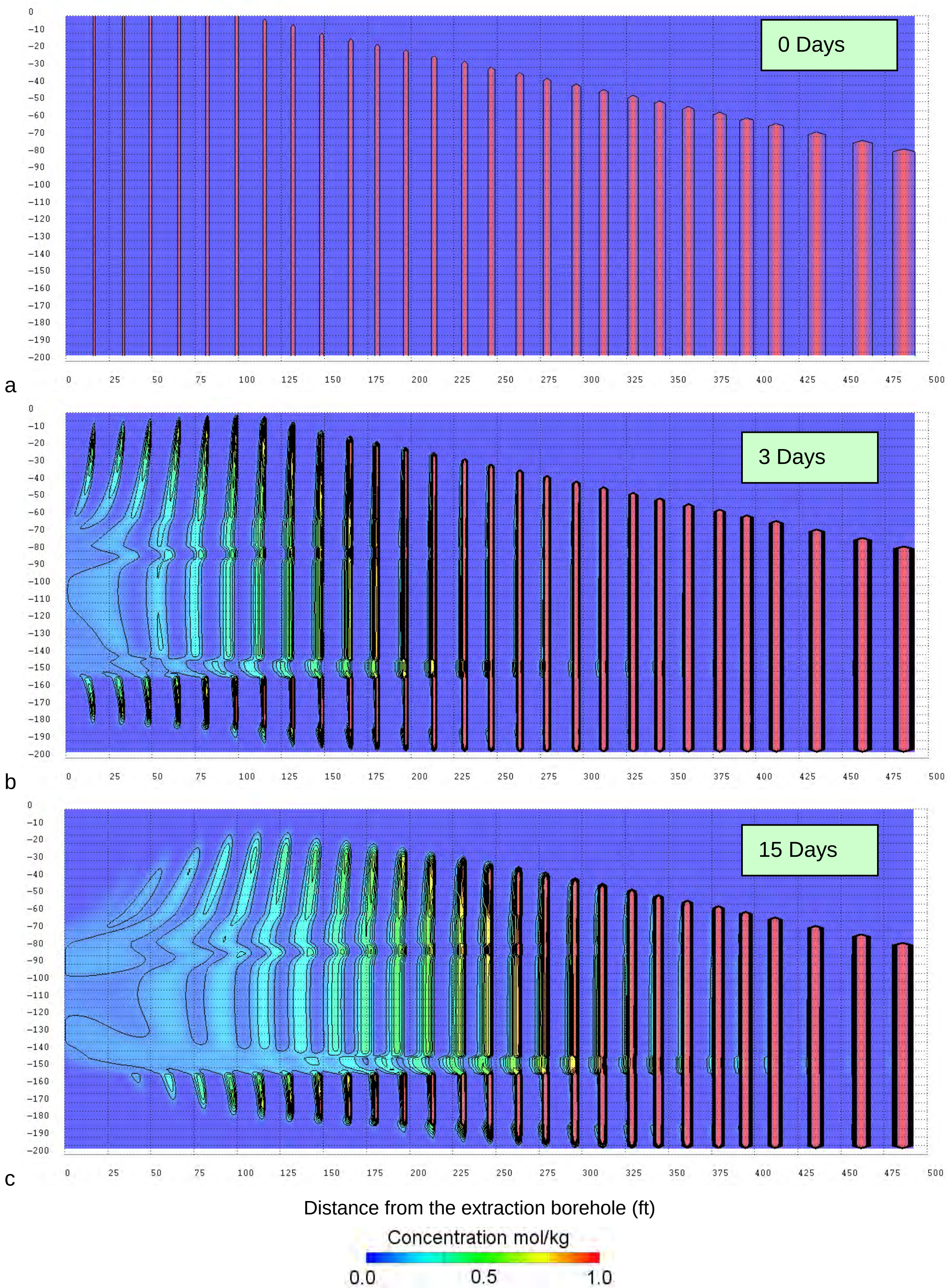

Note: The vertical axis in each of the figures is depth in feet.

Figure 3.3-1 Concentration profiles for visualizing the simulated shallow SVE test from initial conditions at 0 to 60 d of extraction

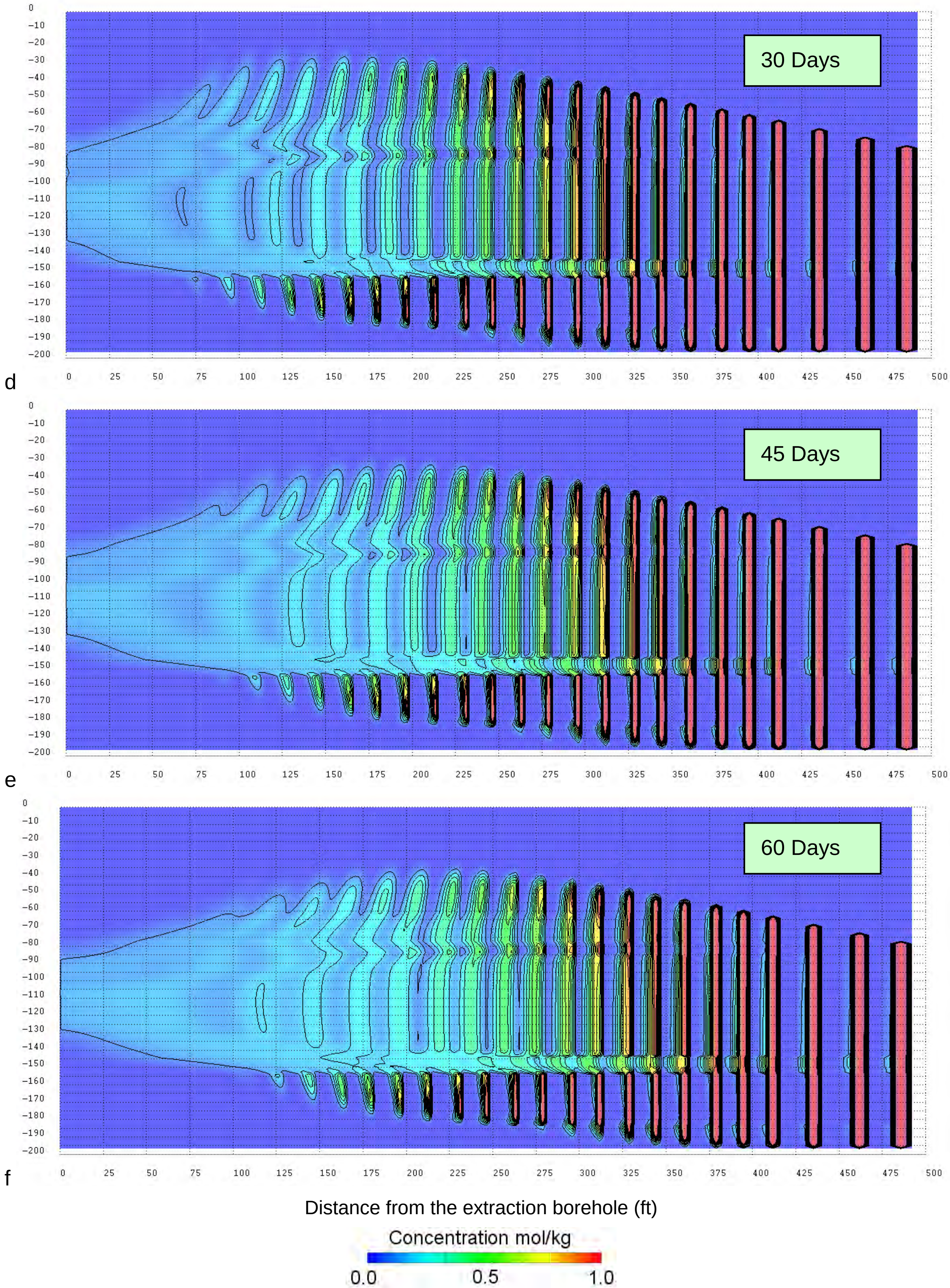

Note: The vertical axis in each of the figures is depth in feet.

Figure 3.3-1 (continued) Concentration profiles for visualizing the simulated shallow SVE test from initial conditions at 0 to 60 d of extraction

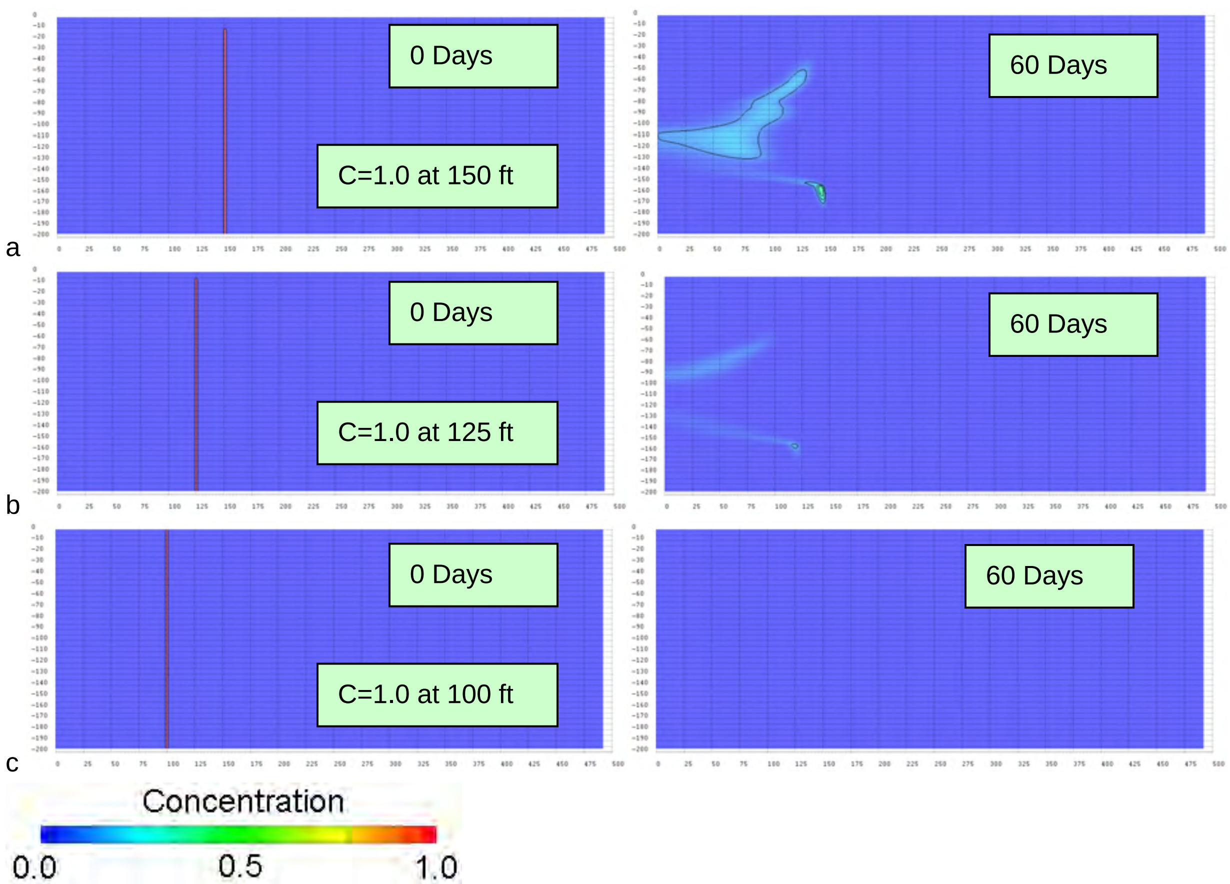

Note: The vertical axis in each of the figures is depth in feet, and the horizontal axis is the distance from the borehole in feet.

Figure 3.3-2 Change in concentrations of tracer bars located at discrete radial distances from the shallow extraction well after 60 d in the simulated shallow SVE test

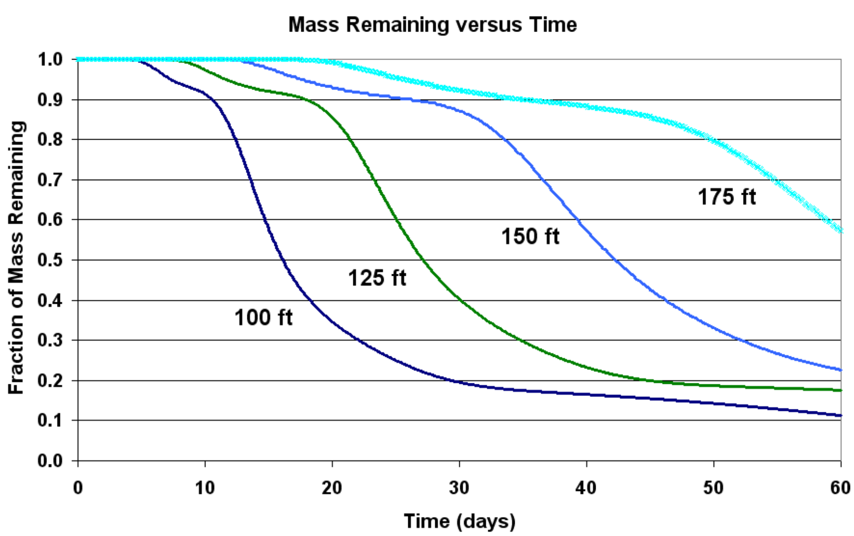

Figure 3.3-3 Mass removal versus time for fixed concentration bars located at 100, 125, 150, and 175 ft from the shallow extraction borehole

3.4 Deep SVE Test ROI

The ROI for the deep SVE test is presented similarly, however with fewer images. Figures 3.4-1a and b show the concentrations left in the domain after only 30 and 60 d.

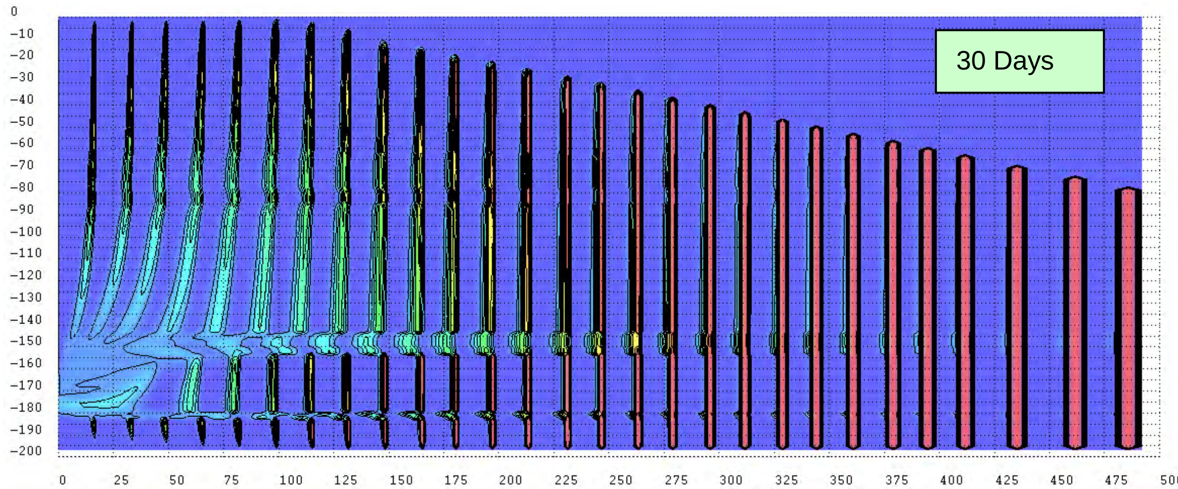

a

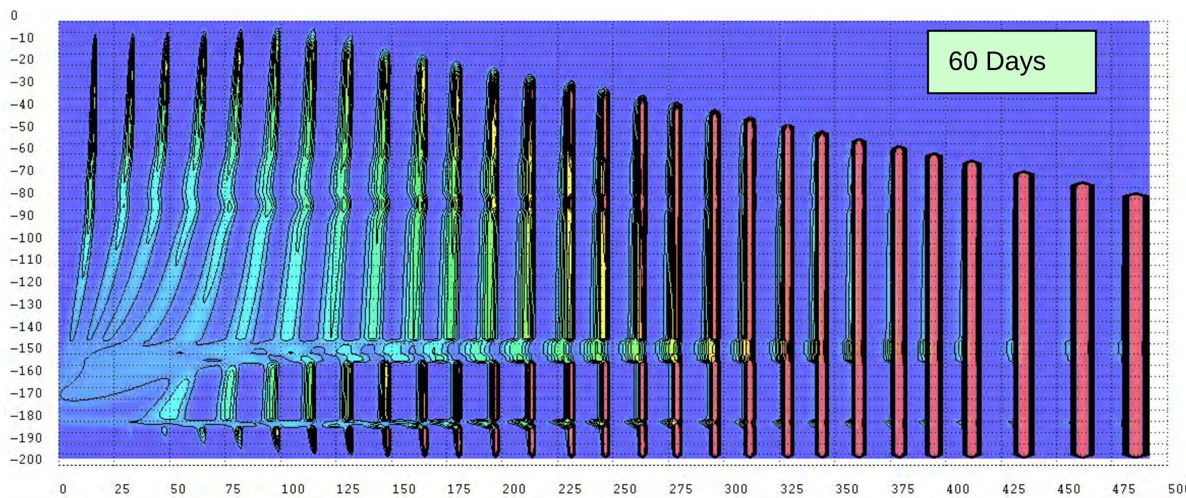

b

Note: The vertical axis in each of the figures is depth in feet, and the horizontal axis is the distance from the borehole in feet.

Figure 3.4-1 Concentration profiles for visualizing the simulated deep SVE test at conditions at 30 d and 60 d of extraction

The figures above show that the extraction pattern is quite different for the deep test. The lower permeability Otowi Member does not allow as much pore-gas flow to the extraction hole. The pressure gradient that results from the permeability distribution begins to pull pore gas preferentially from Qbtt, Qct, and Qbt 1g. To address how this distribution of mass removal relates to an ROI, Figure 3.4-2 shows initial bars of concentration at different distances that are placed in the vertical direction from the base of the model to a depth of only 130 ft.

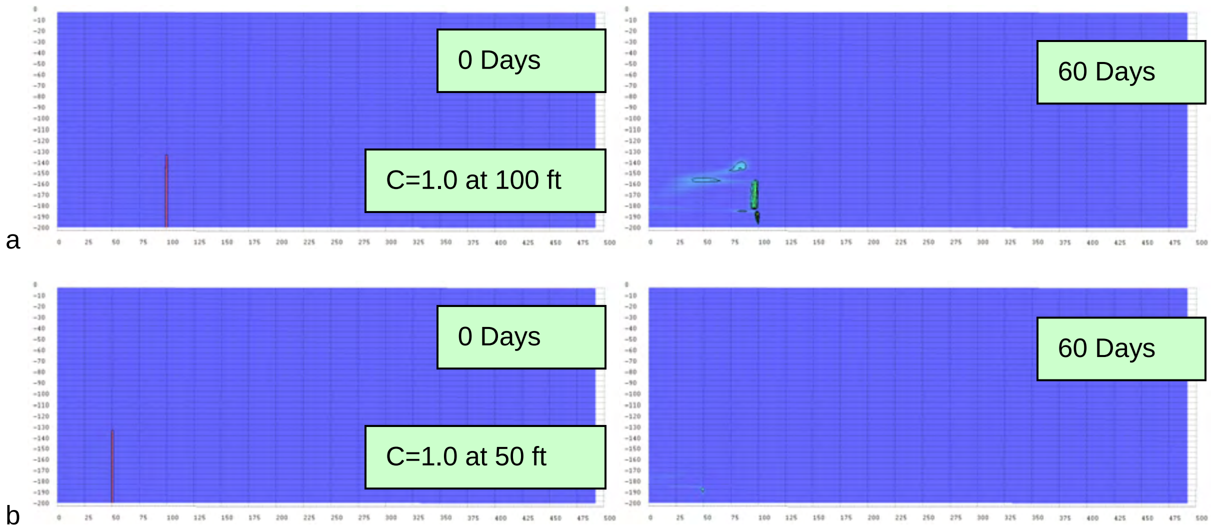

Note: The vertical axis in each of the figures is depth in feet, and the horizontal axis is the distance from the borehole in feet.

Figure 3.4-2 Concentrations for movement of fixed tracer bars for the deep SVE test

Figure 3.4-2a shows that a fixed bar at 100 ft is not removed very efficiently after 60 d, while Figure 3.4-2b shows that a fixed bar at 50 ft is nearly removed in 60 d. Finally, these initial shorter bars can be examined with respect to a percent of the mass remaining at the end of 60 d. Figure 3.4-3 shows that for both 25- and 50-ft initial bars, nearly all the mass is removed, while for a fixed initial bar at 75 ft, only 30% of the original mass is removed. At 100 ft, less than 5% is removed. This series of calculations shows that the ROI for the deep SVE test is on the order of 50 ft.

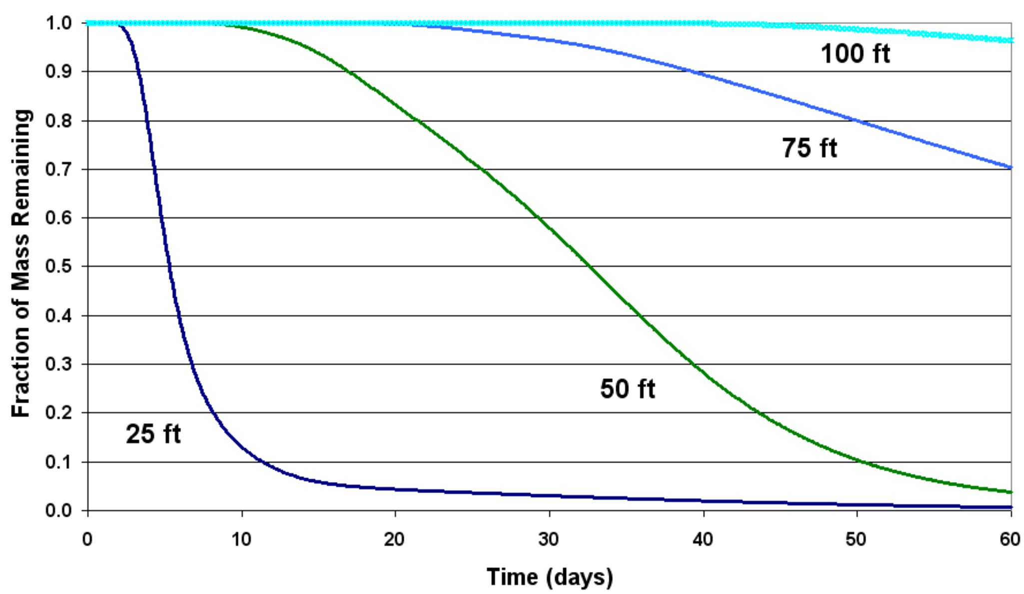

Figure 3.4-3 Mass remaining versus time for fixed tracer bars in the simulated deep SVE test

4.0 CONCLUSIONS

This report uses numerical modeling techniques to better understand the MDA G SVE pilot tests. Initial simulations on a simplified 2-D radial representation of the site were used to determine that the bulk permeability (an average value for all geologic units) in the subsurface at MDA G for the shallow test was on the order of a 6.5 darcies (6.5e–12 m^2), while for the deep test the bulk permeability was closer to 1.3 darcies (1.3e–12 m^2). Next, permeabilities of individual geologic units were modified to simultaneously match the suction and flow rate for both the shallow and deep tests. The permeability structure thus derived was partially validated by comparison of pressure response data in nearby monitoring boreholes to model predictions at the same distances.

Two primary questions were answered with the analysis. First, the results indicate that the relationship between suction and flow rate in both the MDA G shallow and deep SVE tests is likely to be linear, in agreement with results from MDA L. Second, the simulations show that a conservative ROI of the shallow test is on the order of 150 ft and for the deep SVE test is closer to 50 ft. By further quantifying the ROI, this report has shown that the SVE test at MDA G was effective in removing subsurface VOCs.

5.0 REFERENCES

The following list includes all documents cited in this report. Parenthetical information following each reference provides the author(s), publication date, and ER ID. This information is also included in text citations. ER IDs are assigned by the Environmental Programs Directorate's Records Processing Facility (RPF) and are used to locate the document at the RPF and, where applicable, in the master reference set.

Copies of the master reference set are maintained at the NMED Hazardous Waste Bureau and the Directorate. The set was developed to ensure that the administrative authority has all material needed to review this document, and it is updated with every document submitted to the administrative authority. Documents previously submitted to the administrative authority are not included.

EPA (U.S. Environmental Protection Agency), January 26, 2009. "Soil Vapor Extraction (SVE)," Excerpt from EPA 510-B-95-007, Office of Underground Storage Tanks, http://www.epa.gov/oust/cat/SVE1.HTM. (EPA 2009, 104489)

LANL (Los Alamos National Laboratory), October 2007. "Work Plan for the Implementation of an In Situ Soil-Vapor Extraction Pilot Study at Technical Area 54, Material Disposal Area G, Los Alamos National Laboratory," Los Alamos National Laboratory document LA-UR-07-7134, Los Alamos, New Mexico. (LANL 2007, 099777)

LANL (Los Alamos National Laboratory), October 2008. "Pilot Test Report for Evaluating Soil-Vapor Extraction at Material Disposal Area G at Technical Area 54," Los Alamos National Laboratory document LA-UR-08-6883, Los Alamos, New Mexico. (LANL 2008, 103902)

Neeper, D.A., 2002. "Investigation of the Vadose Zone Using Barometric Pressure Cycles," *Journal of Contaminant Hydrology,* Vol. 54, pp. 59-80. (Neeper 2002, 098639)

NMED (New Mexico Environment Department), December 19, 2008. "Notice of Disapproval for the Pilot Test Report for Evaluating Soil-Vapor Extraction at Material Disposal Area G at Technical Area 54," New Mexico Environment Department letter to D. Gregory (DOE-LASO) and D. McInroy (LANL) from J.P. Bearzi (NMED-HWB), Santa Fe, New Mexico. (NMED 2008, 104275)

Stauffer, P.H., K.H. Birdsell, M.S. Witkowski, and J.K. Hopkins, 2005. "Vadose Zone Transport of 1,1,1-Trichloroethane: Conceptual Model Validation through Numerical Simulation," *Vadose Zone Journal,* Vol. 4, pp. 760-773. (Stauffer et al. 2005, 090537)

Stauffer, P.H., J.K. Hopkins, and T. Anderson, February 25–March 1, 2007. "A Soil Vapor Extraction Pilot Study in a Deep Arid Vadose Zone, Part 2: Simulations in Support of Decision Making Processes," Waste Management Conference 2007, February 25–March 1, 2007, Tucson, Arizona. (Stauffer et al. 2007, 104950)

Stauffer, P.H., J.K. Hopkins, T. Anderson, and J. Vrugt, July 11, 2007. "Soil Vapor Extraction Pilot Test at Technical Area 54, Material Disposal Area L: Numerical Modeling in Support of Decision Analysis," Los Alamos National Laboratory document LA-UR-07-4890, Los Alamos, New Mexico. (Stauffer et al. 2007, 097871)

Stauffer, P.H., and N.D. Rosenburg, February 2000. "Vapor Phase Transport at a Hillside Landfill," *Environmental and Engineering Geoscience,* Vol. VI, No. 1, pp. 71–84. (Stauffer and Rosenberg 2000, 104952)

Stauffer, P.H., H.S. Viswanathan, B.A. Robinson, C.W. Gable, G.L. Cole, D.E. Broxton, E.P. Springer, and T.G. Schofield, 2005. "Groundwater Pathway Model for the Los Alamos National Laboratory Technical Area 54, Material Disposal Area G," Los Alamos National Laboratory document LA-UR-05-7393, Los Alamos, New Mexico. (Stauffer et al. 2005, 097432)

Vrugt, J.A., P.H. Stauffer, T. Wöhling, B.A. Robinson, and V.V. Vesselinov, May 2008. "Inverse Modeling of Subsurface Flow and Transport Properties: A Review with New Developments," *Vadose Zone Journal,* Vol. 7, No. 2, pp. 843–864. (Vrugt et al. 2008, 104951)

Zyvoloski, G.A., B.A. Robinson, Z.V. Dash, and L.L. Trease, July 1997. "Summary of the Models and Methods for the FEHM Application — A Finite-Element Heat- and Mass-Transfer Code," Los Alamos National Laboratory report LA-13307-MS, Los Alamos, New Mexico. (Zyvoloski et al. 1997, 070147)